

How Symmetry Governs the Dihedral Angle Dependence of Intermolecular Spin-Orbit Coupling

Antonio J. Garzón-Ramírez, Connor K. Terry Weatherly, Kyle T. Kairys, Michael R. Wasielewski, and Roel Tempelaar*

Department of Chemistry, Institute for Quantum Information Research and Engineering, and Center for Molecular Quantum Transduction, Northwestern University, 2145 Sheridan Road, Evanston, Illinois 60208, USA

E-mail: roel.tempelaar@northwestern.edu

Abstract

Spin-orbit, charge-transfer intersystem crossing (SOCT-ISC) allows for the efficient production of triplet excited states in donor-acceptor (DA) dyads without the involvement of heavy atoms, for use in a myriad of technologies. This process is commonly believed to proceed optimally when the donor and acceptor moieties are oriented under an orthogonal dihedral angle. Here, we challenge this idea through a theoretical study unveiling an orthogonal scenario where spin-orbit couplings (SOCs) are instead minimized. Such is rationalized based on an analysis of the structure-imposed symmetry properties of the involved singlet and triplet states. Notably, in this scenario, finite SOCs demand oblique orientation angles, which in turn requires molecular chirality, suggesting chirality to be a prerequisite for activating the involved SOC pathways.

Introduction

Triplet photosensitizers¹ are useful to many technological applications including photocatalysis,^{2–7} light-emitting diodes,⁸ photovoltaics,^{9–11} photodynamic therapy,^{12–19} and quantum information.^{20,21} In recent years, spin-orbit, charge-transfer intersystem crossing (SOCT-ISC) has received great interest as a pathway for promoting triplet photosensitization in molecular donor-acceptor (DA) dyads.^{22–24} The overall SOCT-ISC process involves photoexcitation into a localized singlet excited state that separates into a charge-transfer state with singlet multiplicity, which is followed by recombination into a localized triplet state.^{25–28} Under favorable conditions, the SOCT-ISC mechanism in-

volves spin-orbit couplings (SOCs) that are orders of magnitude larger than those driving ordinary spin-orbit intersystem crossing between (π, π^*) states,²⁴ enabling high triplet yields in organic molecules without introducing the complications that arise under heavy atom substitutions.^{18,29–32}

It has been argued that SOCs become optimized for an orthogonal dihedral angle between the donor and acceptor moieties,^{25,26,28,33–37} based on a loose analogy to atomic orbital based arguments.^{38,39} Accordingly, the molecular orbitals of the DA dyad being perpendicular creates sufficient orbital angular momentum to induce a change in spin angular momentum upon electron transfer. Yet, systematic investigations of the dihedral angle dependence of SOCT-ISC have remained lacking. Ultimately, the dihedral angle is governed by the structure and sterics of the molecular system and its surroundings.²⁶ As a result, studies have effectively compared angle variations across *different* dyads in order to rationalize changes in SOCs.^{24–26} Among those studies, lack of a clear angle dependence²⁴ as well as efficient SOCT-ISC under non-orthogonal angles have been reported.^{40–44} It remains unclear, however, whether these trends are solely attributable to the relative orientation of the donor and acceptor moieties, or also to variations in the electronic structure across the different dyads. Altogether, this leaves us without a clear picture of how SOCT-ISC can be optimized through tuning the dihedral angle.

Here, we report a computational study of the dihedral-angle dependence of SOCs in donor-acceptor dyads. Through constrained geometry optimizations, we systematically vary the dihedral angle between donor and acceptor dyads. We furthermore present results for which donor and acceptor moieties are sep-

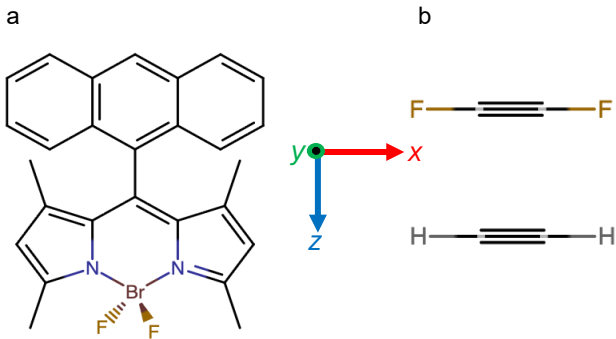


Figure 1: Molecular structure of the dyads studied in this work, BD-anthracene (a) and the idealized system $C_2H_2-C_2F_2$ (b).

arately geometry-optimized, whereupon their nuclear geometries are fused into oriented dyads. Through this route, and by separating out SOC contributions for different polarizations of the triplet spin configuration, we demonstrate that an orthogonal orientation can either enhance *or suppress* the SOCT-ISC mechanism. Results are rationalized by analyzing the structure-imposed symmetries of the involved singlet and triplet states, showing that SOCs can rigorously vanish under orthogonal conditions. These findings open up a framework for the optimization of triplet photosensitizers.

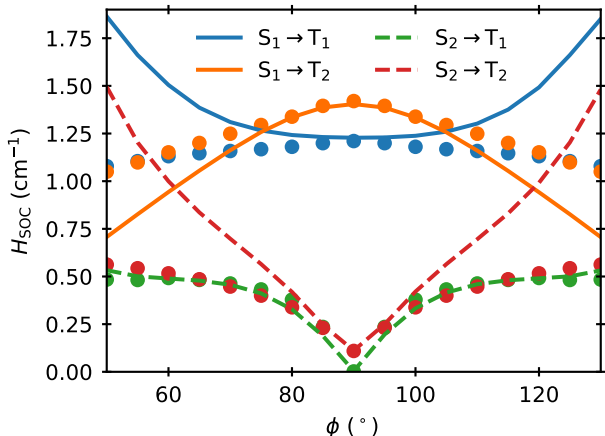


Figure 2: Total SOCs between the two lowest-lying singlet excited states and triplet states as a function of dihedral angle for the BD-anthracene dyad. Shown are results obtained through a constrained geometry optimization of the dyad (markers) and through fusing moieties that were separately geometry-optimized (curves).

Results and Discussion

In our analysis, we pay particular attention to the dyad consisting of boron dipyrromethene (BODIPY or BD) as the donor moiety fused to anthracene as the acceptor moiety, the molecular structure of which is shown in Fig. 1a. The SOCT-ISC mechanism of this dyad was recently studied experimentally by Mani and coworkers.²⁴ The two lowest-lying singlet states of the dyad (S_1 and S_2) are known to be separated by only ~ 0.15 eV,²⁴ and for that reason we include both states in our analysis. Fig. 2 shows calculated total SOCs associated with transitions from S_1 and S_2 to the lowest two triplets (T_1 and T_2), both of which are accessible from either singlet state. The total SOC between the n th singlet state and the m th triplet state is given by

$$H_{\text{SOC}} = \sqrt{\sum_{k=x,y,z} |\langle S_n | \hat{H}_{\text{SOC}} | T_{m,k} \rangle|^2}, \quad (1)$$

where \hat{H}_{SOC} is the spin-orbit coupling Hamiltonian, and $T_{m,k}$ features the index k labeling three orthogonal spin-polarization components of the triplet manifold. Here and henceforth, reported calculations are conducted using PySCF,^{45,46} and invoke time-dependent density functional theory (TD-DFT) within the Tamm-Dancoff approximation, using the PBE50 functional and the 6-311++G** basis set. As seen in Fig. 2, SOCs for each transition are sizable, with values of ~ 1 cm⁻¹, in reasonable agreement with those reported for a fixed ϕ configuration by Mani and coworkers.²⁴

The SOCs shown in Fig. 2 are resolved as a function of the dihedral angle, ϕ , between the BD and anthracene moieties. In common computational approaches, the dihedral angle is subject to the geometry optimization of the overall molecular structure.²⁴ As mentioned, we followed two approaches in order to exert dihedral angle control. In the first approach, a constrained geometry optimization was performed whereby we exclusively controlled the dihedral angle between the donor and acceptor moieties, ϕ . In the second approach, the local nuclear configuration of each moiety was obtained from separate geometry optimizations. These configurations were then fused with a bond length of 1.48 Å and held fixed while the relative orientation of the moieties was varied via the dihedral angle. The latter, hereafter referred to as the Fused Moiety Approach (FMA), allows us to isolate trends in angle-dependent SOCs while minimizing inevitable complications arising under a constrained geometry optimization due to variations in the local moieties structure. Notably, sterics of the dyad restricted the permit-

ted dihedral angle values to $50^\circ < \phi < 130^\circ$, even for the FMA. As seen in Fig. 2, the SOCs calculated within both approaches are in reasonable agreement, especially near $\phi = 90^\circ$ where steric effects are minimal. (Reported calculations were conducted only for $\phi \leq 90^\circ$, as those for $\phi > 90^\circ$ follow trivially upon mirror reflection. All geometry optimizations were conducted in vacuum.)

For both approaches, SOCs are seen to vary significantly with ϕ . Notably, the value for $S_1 \rightarrow T_2$ maximizes at $\phi = 90^\circ$, consistent with predictions made in the literature.^{25,26,28,33–36} However, the three other transitions lack a similar trend, and instead are broadly seen to *minimize* at $\phi = 90^\circ$, with $S_2 \rightarrow T_1$ even vanishing at this angle. These results are inconsistent with the preconception that SOCs are maximized under orthogonality,^{25,26,28,33–36} and warrant further investigation.

There are two factors preventing a deeper investigation based on the BD-anthracene results in Fig. 2. First, the total SOCs given by Eq. 1, although commonly used in calculations of ISC rates, obscure trends manifested in the underlying spin polarizations with $k = x, y$, and z . Second, the limited range of ϕ permitted in the BD-anthracene dyad complicates a comprehensive study of angle-dependent couplings, and prevents study of the zero-angle limit, which is of significance as a point of high symmetry.

We address both limitations by pursuing a polarization-resolved exploration of SOCs for an idealized model dyad. The system of interest is shown in Fig. 1b and consists of two carbon dimers capped with hydrogens and fluorines, C_2H_2 and C_2F_2 , respectively. To simplify this model dyad as much as possible, we subjected it to the FMA, by first conducting a separate geometry optimization of C_2H_2 and C_2F_2 in vacuum. The resulting configurations were then held fixed at a separation of 3.5 Å along an axis normal to the principal axis of each moiety. Even though no covalent bonds are expected to form between the C_2H_2 and C_2F_2 moieties, holding them in close proximity induces bonding-like behavior of their excited states as if bonding occurs, and the dyad thus formed will be referred to as $C_2H_2-C_2F_2$. Notably, the fluorine substitution on one of the carbon dimers introduces a chemical potential difference between the moieties, which avoids resonances that inhibit directed charge transfer.

Shown in Fig. 3 are angle-resolved SOC magnitudes $\langle S_n | \hat{H}_{\text{SOC}} | T_{m,k} \rangle$, for combinations of S_1, S_2, T_1 , and T_2 in $C_2H_2-C_2F_2$, decomposed into polarization-resolved contributions. We define the polarization directions based on the molecular geometry (rather than based on the zero-field splitting tensor used to interpret mag-

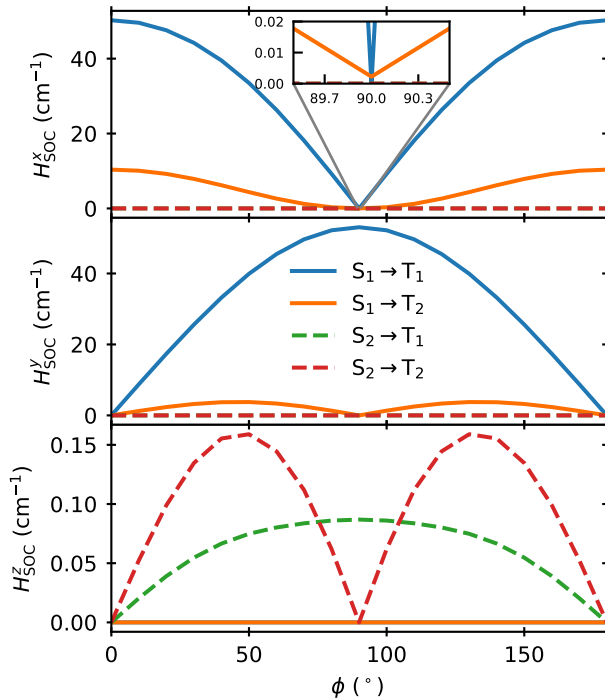


Figure 3: Polarization-resolved SOCs for the two lowest-lying singlet excited states and triplet states as a function of dihedral angle for the idealized dyad $C_2H_2-C_2F_2$.

netic resonance experiments). Specifically, $k = z$ corresponding to the direction along the axis connecting the two moieties, about which the dihedral angle is defined, and the x direction is taken to lie in the plane of the dyad for $\phi = 0^\circ$. Under this angle, we observe extraordinarily large SOCs for $k = x$, which are associated with electron gyration about the principal axes of the C_2H_2 and C_2F_2 moieties. Similar magnitudes are found for $k = y$ under finite angles, as principal axes are tilted out of the xz plane. This effect will vanish for nonlinear moieties such as BD and anthracene. Instead, the $k = z$ component of $C_2H_2-C_2F_2$ involves values that are much more modest, reaching magnitudes in rough agreement with BD-anthracene. Regardless, all polarization-resolved SOCs show clean trends with extreme behaviors at $\phi = 0^\circ$ and $\phi = 90^\circ$ where SOC is maximized, minimized, and at times rigorously zero, broadly consistent with the observations made in Fig. 2 for the total SOCs of BD-anthracene.

Even for the idealized model system $C_2H_2-C_2F_2$, the SOC values are nontrivially governed by many-body electronic interactions. It is therefore difficult to rationalize the SOC values at a quantitative level. However, a qualitative assessment can be conducted based on the symmetry properties of the involved singlet and

Table 1: Dihedral-angle dependent irreps of the two lowest-lying singlet excited states and triplet states of $C_2H_2-C_2F_2$. Shown below are flags indicating whether or not SOCs are symmetry-allowed.

ϕ	0°			45°			90°		
k	x	y	z	x	y	z	x	y	z
S_1	A ₂	A ₂	A ₂	A	A	A	A ₂	A ₂	A ₂
S_2	B ₁	B ₁	B ₁	B	B	B	B ₁	B ₁	B ₁
$T_{1,k}$	A ₂	A ₁	B ₂	A	A	B	A ₁	A ₂	B ₁
$T_{2,k}$	A ₂	A ₁	B ₂	A	A	B	A ₂	A ₁	B ₂
$S_1 \rightarrow T_{1,k}$	✓	✗	✗	✓	✓	✗	✗	✓	✗
$S_1 \rightarrow T_{2,k}$	✓	✗	✗	✓	✓	✗	✓	✗	✗
$S_2 \rightarrow T_{1,k}$	✗	✗	✗	✗	✗	✓	✗	✗	✓
$S_2 \rightarrow T_{2,k}$	✗	✗	✗	✗	✗	✓	✗	✗	✗

triplet states. Notably, within the FMA we arrive at molecular structures with idealized symmetry properties, which translates to highly-symmetric electronic excitations. This permits a symmetry analysis based on which to establish principles for intermolecular SOC in analogy to the heuristic atomic orbital rules for intramolecular SOC proposed by El-Sayed.³⁸ Specifically, for SOC to be nonzero, $\langle S_n | \hat{H}_{SOC} | T_{m,k} \rangle \neq 0$, it is required that the tensor product of the irreducible representations (irreps) of the involved states S_n and $T_{m,k}$, and the SOC Hamiltonian, \hat{H}_{SOC} , is contained in the totally-symmetric irrep (Γ_s) of the point group of the dyad. That is,^{47,48}

$$\Gamma(S_n) \otimes \Gamma(\hat{H}_{SOC}) \otimes \Gamma(T_{m,k}) \supset \Gamma_s, \quad (2)$$

where $\Gamma(i)$ denotes the irrep of quantity i . Given that $\Gamma(\hat{H}_{SOC}) = \Gamma_s$, this is equivalent to $\Gamma(S_n) \otimes \Gamma(T_{m,k}) \supset \Gamma_s$. We note that, in our analysis, S_n and $T_{m,k}$ are taken to represent spin and spatial product states, and the operator \hat{H}_{SOC} is retained in the full spin-orbit basis.

The symmetry of the dyadic structure depends on the dihedral angle, for which three cases can be differentiated. Two singular cases correspond to $\phi = 0^\circ$ and 90° , where the structure reaches distinct symmetries. This contrasts with the generic case of an oblique dihedral angle, $0 < \phi < 90^\circ$, for which the symmetry tends to be lower. (Here and henceforth, we will restrict the discussion to $0 \leq \phi \leq 90^\circ$ while noting that the domain $90 \leq \phi \leq 180^\circ$ follows trivially upon mirror reflection.) These principles impact the electronic state symmetry, as becomes obvious in Table 1, which shows the Mulliken symbols for the irreps of the two lowest-lying singlet excited states and triplet states of $C_2H_2-C_2F_2$ for $\phi = 0^\circ$ and 90° , as well as an oblique angle value $\phi = 45^\circ$. The irreps allow us to assess whether or not SOCs are allowed by symmetry for combinations of the

states involved, as established by Eq. 2.

Included in Table 1 are flags indicating whether or not SOCs are symmetry-allowed. Critically, instances where this analysis predicts SOCs to be symmetry-forbidden all correspond to vanishing coupling values in Fig. 3. Furthermore, this figure shows that coupling values typically undergo monotonic growth towards extrema across regions where SOCs are symmetry-allowed. Notably, there are also transitions for which SOCs are forbidden throughout all ϕ values, which is reflected both in Fig. 3 and Table 1. As such, we find the symmetry analysis to account for the behavior of the spin-polarization resolved SOCs.

We proceed to apply a similar symmetry analysis to the BD-anthracene dyad, while defining the polarization directions analogously. (As with $C_2H_2-C_2F_2$, we first restrict ourselves to the FMA, since a constrained geometry optimization of the entire dyad entails subtle symmetry breaking, producing a low-symmetry conformation that does not permit a meaningful symme-

Table 2: Dihedral-angle dependent irreps for the two lowest-lying singlet excited states and triplet states of the BD-anthracene dyad. Shown below are flags indicating whether or not SOCs are symmetry-allowed.

ϕ	50°			90°		
k	x	y	z	x	y	z
S_1	A	A	A	A ₂	A ₂	A ₂
S_2	B	B	B	B ₂	B ₂	B ₂
$T_{1,k}$	A	A	B	A ₁	A ₂	B ₁
$T_{2,k}$	B	B	A	B ₂	B ₁	A ₂
$S_1 \rightarrow T_{1,k}$	✓	✓	✗	✗	✓	✗
$S_1 \rightarrow T_{2,k}$	✗	✗	✓	✗	✗	✓
$S_2 \rightarrow T_{1,k}$	✗	✗	✓	✗	✗	✗
$S_2 \rightarrow T_{2,k}$	✓	✓	✗	✓	✗	✗

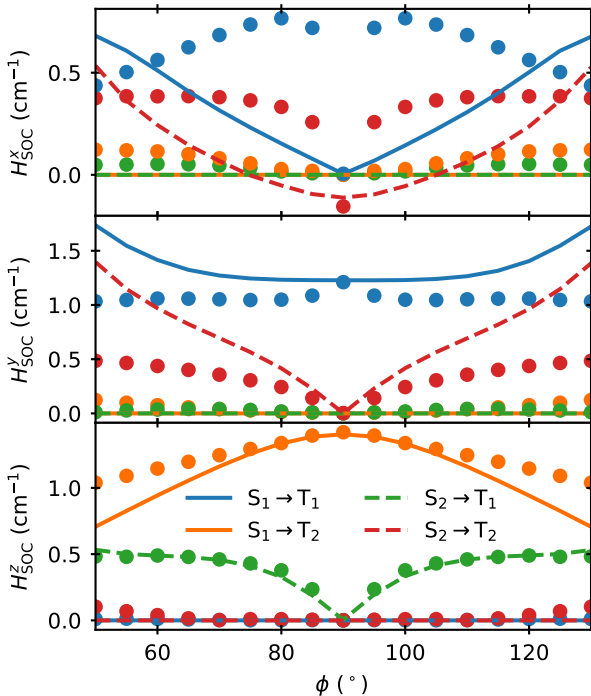


Figure 4: As in Fig. 2, but for polarization-resolved SOC strengths.

try analysis.) Results are summarized in Table 2 for $\phi = 50^\circ$ and 90° , which represent physically-relevant dihedral angle values permitted by the sterics of the dyad. As with $C_2H_2-C_2F_2$, we observe various combinations of transitions and angles where SOC strengths are symmetry-forbidden, which we expect to bear out in the SOC calculations. To assess this, we show in Fig. 4 the polarization-resolved SOC strengths between the two lowest-lying singlet excited states and triplet states of BD-anthracene. Results are shown from the FMA as well as the constrained geometry optimization, the former of which should match the behavior predicted by Table 2. Indeed, any instance marked as symmetry-forbidden in Table 2 manifest as a rigorously-vanishing value in the calculated SOC strengths. Notably, however, the $S_2 \rightarrow T_{2,x}$ transition is seen to cross a zero value at an oblique angle of $\phi \sim 75^\circ$. This illustrates that the symmetry analysis provides a necessary but not sufficient criterion for SOC strengths to be nonzero. In Fig. 4, SOC strengths calculated under the constrained geometry optimization are seen to be in reasonable agreement with those from the FMA, with differences at small angles attributable to steric effects, and deviations close to perpendicular conditions being attributable to symmetry breaking arising under the constrained geometry optimization.

The total SOC strengths shown in Fig. 2 follow from the polarization-resolved contributions from Fig. 4 through

substitution into Eq. 1, and the total SOC strengths can therefore be understood based on those contributions. In turn, any instance of nonvanishing contributions are rationalized by the symmetry analysis from Table 2. Notably, the coupling associated with $S_2 \rightarrow T_1$ is symmetry-forbidden at $\phi = 90^\circ$ for all spin polarizations ($k = x, y, \text{ and } z$). Similar behavior is observed for $S_2 \rightarrow T_2$ in $C_2H_2-C_2F_2$. For this ideal model dyad, the lack of steric restrictions allows the dihedral angle to be scanned throughout, permitting us to make a remarkable observation: For the $S_2 \rightarrow T_2$ SOC to be symmetry-allowed, the dyad needs to be oriented such that the dihedral angle is oblique.

Curiously, the oblique dihedral angle, required for certain singlet-triplet transitions to become symmetry-allowed, effectively renders the dyad chiral. It can thus be concluded that chirality is a fundamental requisite for the associated SOC to become activated. This in turn suggests a profound connection between spin effects and chirality, which resonates with the recent surge in studies also suggesting this connection.^{49–51} Notably, the spin polarization for which SOC becomes activated aligns with the axis connecting the donor and acceptor moieties, about which the dihedral angle is defined. Altogether, this principle shows consistency with the experimental observation of increased T_z populations upon the introduction of chirality in donor-bridge-acceptor triads.⁵¹

Conclusion

To conclude, we have explored SOC strengths between low-lying singlet and triplet states in two donor-acceptor dyads, with the aim to elucidate the principles driving SOCT-ISC. We have compared two approaches wherein geometry optimizations were applied to the entire dyad (while constraining the dihedral angle) versus the individual moieties, in order to systematically study dihedral angle dependence of SOC strengths. We have shown that spin-polarization resolved SOC strengths are well accounted for by a symmetry analysis, establishing a framework analogous to the El-Sayed rules, but at the intermolecular level. This framework could be helpful for ongoing efforts to engineer excited-state dynamics by tuning the dihedral angle in dyads.⁵² It rationalizes that SOC strengths could be maximized or minimized under an orthogonal angle, depending on the singlet and triplet state symmetries. It furthermore suggests a critical connection between SOC strengths and chirality for certain singlet-triplet transitions.

Acknowledgements

This work was supported as part of the Center for Molecular Quantum Transduction, an Energy Frontier Research Center funded by the U.S. Department of Energy, Office of Science, Basic Energy Sciences, under Award #DE-SC0021314.

References

- (1) Zhao, J.; Wu, W.; Sun, J.; Guo, S. Triplet photosensitizers: from molecular design to applications. *Chemical Society Reviews* **2013**, *42*, 5323.
- (2) Shi, L.; Xia, W. Photoredox functionalization of C–H bonds adjacent to a nitrogen atom. *Chemical Society Reviews* **2012**, *41*, 7687.
- (3) Xuan, J.; Xiao, W. Visible-Light Photoredox Catalysis. *Angewandte Chemie International Edition* **2012**, *51*, 6828–6838.
- (4) Hari, D. P.; König, B. The Photocatalyzed Meerwein Arylation: Classic Reaction of Aryl Diazonium Salts in a New Light. *Angewandte Chemie International Edition* **2013**, *52*, 4734–4743.
- (5) Hari, D. P.; König, B. Synthetic applications of eosin Y in photoredox catalysis. *Chem. Commun.* **2014**, *50*, 6688–6699.
- (6) Schultz, D. M.; Yoon, T. P. Solar Synthesis: Prospects in Visible Light Photocatalysis. *Science* **2014**, *343*, 1239176.
- (7) Gunderson, V. L.; Krieg, E.; Vagnini, M. T.; Iron, M. A.; Rybtchinski, B.; Wasielewski, M. R. Photoinduced Singlet Charge Transfer in a Ruthenium(II) Perylene-3,4:9,10-bis(dicarboximide) Complex. *The Journal of Physical Chemistry B* **2011**, *115*, 7533–7540.
- (8) Baldo, M. A.; O'Brien, D. F.; You, Y.; Shoustikov, A.; Sibley, S.; Thompson, M. E.; Forrest, S. R. Highly efficient phosphorescent emission from organic electroluminescent devices. *Nature* **1998**, *395*, 151–154.
- (9) Dai, F.; Zhan, H.; Liu, Q.; Fu, Y.; Li, J.; Wang, Q.; Xie, Z.; Wang, L.; Yan, F.; Wong, W. Platinum(II)–Bis(aryleneethynylene) Complexes for Solution-Processible Molecular Bulk Heterojunction Solar Cells. *Chemistry – A European Journal* **2012**, *18*, 1502–1511.
- (10) Congreve, D. N.; Lee, J.; Thompson, N. J.; Hontz, E.; Yost, S. R.; Reuswig, P. D.; Bahlke, M. E.; Reineke, S.; Van Voorhis, T.; Baldo, M. A. External Quantum Efficiency Above 100% in a Singlet-Exciton-Fission–Based Organic Photovoltaic Cell. *Science* **2013**, *340*, 334–337.
- (11) Suzuki, S.; Matsumoto, Y.; Tsubamoto, M.; Sugimura, R.; Kozaki, M.; Kimoto, K.; Iwamura, M.; Nozaki, K.; Senju, N.; Uragami, C.; Hashimoto, H.; Muramatsu, Y.; Konno, A.; Okada, K. Photoinduced electron transfer of platinum(ii) bipyridine diacetylides linked by triphenylamine- and naphthaleneimide-derivatives and their application to photoelectric conversion systems. *Physical Chemistry Chemical Physics* **2013**, *15*, 8088.
- (12) Cló, E.; Snyder, J. W.; Ogilby, P. R.; Gothelf, K. V. Control and Selectivity of Photosensitized Singlet Oxygen Production: Challenges in Complex Biological Systems. *ChemBioChem* **2007**, *8*, 475–481.
- (13) Celli, J. P.; Spring, B. Q.; Rizvi, I.; Evans, C. L.; Samkoe, K. S.; Verma, S.; Pogue, B. W.; Hasan, T. Imaging and Photodynamic Therapy: Mechanisms, Monitoring, and Optimization. *Chemical Reviews* **2010**, *110*, 2795–2838.
- (14) Awuah, S. G.; You, Y. Boron dipyrromethene (BODIPY)-based photosensitizers for photodynamic therapy. *RSC Advances* **2012**, *2*, 11169.
- (15) Kamkaew, A.; Lim, S. H.; Lee, H. B.; Kiew, L. V.; Chung, L. Y.; Burgess, K. BODIPY dyes in photodynamic therapy. *Chem. Soc. Rev.* **2013**, *42*, 77–88.
- (16) Stacey, O. J.; Pope, S. J. A. New avenues in the design and potential application of metal complexes for photodynamic therapy. *RSC Advances* **2013**, *3*, 25550.
- (17) Weijer, R.; Broekgaarden, M.; Kos, M.; Van Vught, R.; Rauws, E. A.; Breukink, E.; Van Gulik, T. M.; Storm, G.; Heger, M. Enhancing photodynamic therapy of refractory solid cancers: Combining second-generation photosensitizers with multi-targeted liposomal delivery. *Journal of Photochemistry and Photobiology C: Photochemistry Reviews* **2015**, *23*, 103–131.

- (18) Zhao, J.; Xu, K.; Yang, W.; Wang, Z.; Zhong, F. The triplet excited state of Bodipy: formation, modulation and application. *Chemical Society Reviews* **2015**, *44*, 8904–8939.
- (19) Li, X.; Kolemen, S.; Yoon, J.; Akkaya, E. U. Activatable Photosensitizers: Agents for Selective Photodynamic Therapy. *Advanced Functional Materials* **2017**, *27*, 1604053.
- (20) Attwood, M.; Li, Y.; Nevjestic, I.; Diggle, P.; Colauto, A.; Betala, M.; White, A. J. P.; Oxborrow, M. Probing the Design Rules for Optimizing Electron Spin Relaxation in Densely Packed Triplet Media for Quantum Applications. *ACS Materials Letters* **2025**, *7*, 286–294.
- (21) Palmer, J. R.; Williams, M. L.; Young, R. M.; Peinkofer, K. R.; Phelan, B. T.; Krzyaniak, M. D.; Wasielewski, M. R. Oriented Triplet Excitons as Long-Lived Electron Spin Qutrits in a Molecular Donor–Acceptor Single Cocrystal. *Journal of the American Chemical Society* **2024**, *146*, 1089–1099.
- (22) Zhao, J.; Chen, K.; Hou, Y.; Che, Y.; Liu, L.; Jia, D. Recent progress in heavy atom-free organic compounds showing unexpected intersystem crossing (ISC) ability. *Organic & Biomolecular Chemistry* **2018**, *16*, 3692–3701.
- (23) Hou, Y.; Zhang, X.; Chen, K.; Liu, D.; Wang, Z.; Liu, Q.; Zhao, J.; Barbon, A. Charge separation, charge recombination, long-lived charge transfer state formation and intersystem crossing in organic electron donor/acceptor dyads. *Journal of Materials Chemistry C* **2019**, *7*, 12048–12074.
- (24) Buck, J. T.; Boudreau, A. M.; DeCarminé, A.; Wilson, R. W.; Hampsey, J.; Mani, T. Spin-Allowed Transitions Control the Formation of Triplet Excited States in Orthogonal Donor–Acceptor Dyads. *Chem* **2019**, *5*, 138–155.
- (25) Okada, T.; Karaki, I.; Matsuzawa, E.; Mataga, N.; Sakata, Y.; Misumi, S. Ultrafast intersystem crossing in some intramolecular heteroexcimers. *The Journal of Physical Chemistry* **1981**, *85*, 3957–3960.
- (26) Van Willigen, H.; Jones, G.; Farahat, M. S. Time-Resolved EPR Study of Photoexcited Triplet-State Formation in Electron-Donor-Substituted Acridinium Ions. *The Journal of Physical Chemistry* **1996**, *100*, 3312–3316.
- (27) Gould, I. R.; Boiani, J. A.; Gaillard, E. B.; Goodman, J. L.; Farid, S. Intersystem Crossing in Charge-Transfer Excited States. *The Journal of Physical Chemistry A* **2003**, *107*, 3515–3524.
- (28) Dance, Z. E. X.; Mi, Q.; McCamant, D. W.; Ahrens, M. J.; Ratner, M. A.; Wasielewski, M. R. Time-Resolved EPR Studies of Photogenerated Radical Ion Pairs Separated by *p*-Phenylene Oligomers and of Triplet States Resulting from Charge Recombination. *The Journal of Physical Chemistry B* **2006**, *110*, 25163–25173.
- (29) Yogo, T.; Urano, Y.; Ishitsuka, Y.; Maniwa, F.; Nagano, T. Highly Efficient and Photostable Photosensitizer Based on BODIPY Chromophore. *Journal of the American Chemical Society* **2005**, *127*, 12162–12163.
- (30) Adarsh, N.; Avirah, R. R.; Ramaiah, D. Tuning Photosensitized Singlet Oxygen Generation Efficiency of Novel Aza-BODIPY Dyes. *Organic Letters* **2010**, *12*, 5720–5723.
- (31) Sabatini, R. P.; McCormick, T. M.; Lazarides, T.; Wilson, K. C.; Eisenberg, R.; McCamant, D. W. Intersystem Crossing in Halogenated Bodipy Chromophores Used for Solar Hydrogen Production. *The Journal of Physical Chemistry Letters* **2011**, *2*, 223–227.
- (32) Wu, W.; Guo, H.; Wu, W.; Ji, S.; Zhao, J. Organic Triplet Sensitizer Library Derived from a Single Chromophore (BODIPY) with Long-Lived Triplet Excited State for Triplet–Triplet Annihilation Based Upconversion. *The Journal of Organic Chemistry* **2011**, *76*, 7056–7064.
- (33) Wang, Z.; Zhao, J. Bodipy–Anthracene Dyads as Triplet Photosensitizers: Effect of Chromophore Orientation on Triplet-State Formation Efficiency and Application in Triplet–Triplet Annihilation Upconversion. *Organic Letters* **2017**, *19*, 4492–4495.
- (34) Sartor, S. M.; McCarthy, B. G.; Pearson, R. M.; Miyake, G. M.; Damrauer, N. H. Exploiting Charge-Transfer States for Maximizing Intersystem Crossing Yields in Organic Photoredox Catalysts. *Journal of the American Chemical Society* **2018**, *140*, 4778–4781.
- (35) Liu, Y.; Zhao, J.; Iagatti, A.; Bussotti, L.; Foggi, P.; Castellucci, E.; Di Donato, M.;

- Han, K.-L. A Revisit to the Orthogonal Bodipy Dimers: Experimental Evidence for the Symmetry Breaking Charge Transfer-Induced Intersystem Crossing. *The Journal of Physical Chemistry C* **2018**, *122*, 2502–2511.
- (36) Dong, Y.; Taddei, M.; Doria, S.; Bussotti, L.; Zhao, J.; Mazzone, G.; Di Donato, M. Torsion-Induced Nonradiative Relaxation of the Singlet Excited State of *meso*-Thienyl Bodipy and Charge Separation, Charge Recombination-Induced Intersystem Crossing in Its Compact Electron Donor/Acceptor Dyads. *The Journal of Physical Chemistry B* **2021**, *125*, 4779–4793.
- (37) Aster, A.; Rumble, C.; Bornhof, A.-B.; Huang, H.-H.; Sakai, N.; Šolomek, T.; Matile, S.; Vauthey, E. Long-lived triplet charge-separated state in naphthalenediimide based donor–acceptor systems. *Chemical Science* **2021**, *12*, 4908–4915.
- (38) El-Sayed, M. A. Spin–Orbit Coupling and the Radiationless Processes in Nitrogen Heterocyclics. *The Journal of Chemical Physics* **1963**, *38*, 2834–2838.
- (39) El-Sayed, M. A. Triplet state. Its radiative and nonradiative properties. *Accounts of Chemical Research* **1968**, *1*, 8–16.
- (40) Hou, Y.; Kurganskii, I.; Elmali, A.; Zhang, H.; Gao, Y.; Lv, L.; Zhao, J.; Karatay, A.; Luo, L.; Fedin, M. Electronic coupling and spin–orbit charge transfer intersystem crossing (SOCT-ISC) in compact BDP–carbazole dyads with different mutual orientations of the electron donor and acceptor. *The Journal of Chemical Physics* **2020**, *152*, 114701.
- (41) Rehmat, N.; Toffoletti, A.; Mahmood, Z.; Zhang, X.; Zhao, J.; Barbon, A. Carbazole-perylenebisimide electron donor/acceptor dyads showing efficient spin orbit charge transfer intersystem crossing (SOCT-ISC) and photo-driven intermolecular electron transfer. *Journal of Materials Chemistry C* **2020**, *8*, 4701–4712.
- (42) Xu, J.; Zeng, H.; Wang, K.; Peng, S.; Chen, X.; Zhang, Y.; Wu, D.; Xia, J. High-Yield Triplet States from Charge-Transfer-Mediated Intersystem Crossing in a Thionated Perylene Dimer. *The Journal of Physical Chemistry C* **2024**, *128*, 20967–20973.
- (43) Williams, M. L.; Schlesinger, I.; Jacobberger, R. M.; Wasielewski, M. R. Mechanism of Ultrafast Triplet Exciton Formation in Single Cocrystals of π -Stacked Electron Donors and Acceptors. *Journal of the American Chemical Society* **2022**, *144*, 18607–18618.
- (44) Williams, M. L.; Palmer, J. R.; Tyndall, S. B.; Chen, Y.; Young, R. M.; Garzon-Ramirez, A. J.; Tempelaar, R.; Wasielewski, M. R. Molecular engineering charge transfer and triplet exciton formation in donor–acceptor cocrystals. *The Journal of Chemical Physics* **2025**, *162*, 024505.
- (45) Sun, Q.; Berkelbach, T. C.; Blunt, N. S.; Booth, G. H.; Guo, S.; Li, Z.; Liu, J.; McClain, J. D.; Sayfutyarova, E. R.; Sharma, S.; Wouters, S.; Chan, G. K. P. SCF: the Python-based simulations of chemistry framework. *WIREs Computational Molecular Science* **2018**, *8*, e1340.
- (46) Sun, Q. et al. Recent developments in the P SCF program package. *The Journal of Chemical Physics* **2020**, *153*, 024109.
- (47) WIGNER, E. P., Ed. *Group Theory*; Pure and Applied Physics; Elsevier, 1959; Vol. 5; pp 373–374.
- (48) Marian, C. M. In *Reviews in Computational Chemistry*, 1st ed.; Lipkowitz, K. B., Boyd, D. B., Eds.; Wiley, 2001; Vol. 17; pp 99–204.
- (49) Ray, K.; Ananthavel, S. P.; Waldeck, D. H.; Naaman, R. Asymmetric Scattering of Polarized Electrons by Organized Organic Films of Chiral Molecules. *Science* **1999**, *283*, 814–816.
- (50) Naaman, R.; Paltiel, Y.; Waldeck, D. H. Chiral molecules and the electron spin. *Nature Reviews Chemistry* **2019**, *3*, 250–260.
- (51) Eckvahl, H. J.; Tcyrulnikov, N. A.; Chiesa, A.; Bradley, J. M.; Young, R. M.; Carretta, S.; Krzyaniak, M. D.; Wasielewski, M. R. Direct observation of chirality-induced spin selectivity in electron donor–acceptor molecules. *Science* **2023**, *382*, 197–201.
- (52) Estergreen, L.; Mencke, A. R.; Cotton, D. E.; Korovina, N. V.; Michl, J.; Roberts, S. T.; Thompson, M. E.; Bradforth, S. E. Controlling Symmetry Breaking Charge Transfer in BODIPY Pairs.

Accounts of Chemical Research **2022**, 55, 1561–1572.